Hydrothermal Synthesis, Structure Determination, and Magnetic Properties of a New Layered Oxyfluorinated Iron Phosphate Templated by 1,4-Diaminobutane

Myriam Riou-Cavellec,* Jean-Marc Grenèche,† Didier Riou, and Gérard Férey

Institut Lavoisier, UMR CNRS C173, Université de Versailles-St Quentin en Yv., 45 Av. des Etats-Unis, 78035 Versailles, France, and Laboratoire de Physique de l'Etat Condensé, UPRES A 6087, Université du Maine, Av. Olivier Messiaen, 72085 Le Mans Cedex 9, France

Received February 26, 1998. Revised Manuscript Received May 13, 1998

$[Fe^{III}_5F_3(PO_4)_6(H_2O)_3](H_2O)_2\cdot(H_3N(CH_2)_4NH_3)_3$ (labeled MIL-4) was synthesized hydrothermally from a mixture of Fe_2O_3:P_2O_5:HF:1,4-diaminobutane:H_2O in the molar ratio 1:1:2:1.5:80. Its structure was solved by single-crystal X-ray diffraction in the noncentrosymmetric orthorhombic space group $P2_12_12_1$ (No. 19) with lattice parameters a = 9.5852(1) Å, b = 15.5879(3) Å, c = 29.2556(2) Å, V = 4371.2(1) Å^3, Z = 4. MIL-4 is a layered compound whose inorganic layers are characterized by the presence of helicoidal chains of $Fe^{III}X_6$ (X = O, H_2O, F) corner-shared octahedra. The organic cations located between the layers ensure both the electroneutrality of the compound and the stability of the framework by strong hydrogen bonds. The magnetic measurements show that MIL-4 exhibits a ferrimagnetic behavior under T_C = 7(1) K.

Introduction

A large number of alumino and gallophosphates with open-structures have been synthesized under mild conditions using organic amines as structure-directing agents.[1] By adding fluorhydric acid in the synthesis medium, Guth and Kessler[2] showed that fluorine (i) acts as a good mineralizor and (ii) allows for neutral or acidic conditions and thus leads to new structural types including the fluorine to the inorganic framework. The most famous examples were first the cloverite[3] and then the ULM-*n* family ($n \leqslant 19$).[4] From the structural study of the alumino and gallophosphates with ULM type, we have proposed a hypothesis for a mechanism of formation of these phases.[5] This mechanism claims that the building units observed in the final solid exist in the solution, the size of these oligomers being controlled by the charge density of the amine. The solid is then formed by the infinite condensation of the neutral ion pairs constituted by the polyhedral oligomers and the protonated amines. This proposition has just received its first experimental confirmations by in situ NMR experiments under hydrothermal conditions.[6] In this hypothesis, the chemical nature of the metal seems minor and suggests the possibility to completely substitute the aluminum or gallium atoms by a 3d transition metal. In this way, we have succeeded in the synthesis of iron phosphates with ULM-3,[7] ULM-4,[8] and ULM-11[9] topologies (these latter were first synthesized with Al^{3+} or Ga^{3+}), but we also obtained new iron compounds with three-dimensional open frameworks labeled ULM-15,[10] ULM-12,[11] and ULM-19.[12] Several papers of Lii[13−15] and Haushalter[16] published later are devoted to iron phosphates with open structures, but the iron ULM compounds are the first oxyfluorinated microporous compounds with magnetic properties.

This papers deals with the synthesis, structure determination, and magnetic properties of a new layered oxyfluorinated ferric phosphate templated by 1,4-diaminobutane named MIL-4 (Materials of Institut Lavoisier n*o*. 4).

Experimental Section

1. Synthesis. $[Fe_5F_3(PO_4)_6(H_2O)_3](H_2O)_2\cdot(N_2C_4H_{14})_3$ was synthesized hydrothermally from a mixture of Fe_2O_3 (Aldrich,

* To whom correspondence should be addressed.
† Université du Maine.

(1) Wilson, S. T.; Lok, B. M.; Messina, C. A.; Cannan, T. R.; Flanigen, E. M. *J. Am. Chem. Soc.* **1982**, *104*, 1146.
(2) Guth, J. L.; Kessler, H.; Wey, R. *Stud. Surf. Sci. Catal.* **1986**, *28*, 121.
(3) Estermann, M.; McCusker, L. B.; Baerlocher, C.; Merrouche, A.; Kessler, H. *Nature* **1991**, *352*, 320.
(4) Loiseau, T., Ph.D. Thesis, Université du Maine (Le Mans); France, 1994.
(5) Férey, G. *J. Fluorine Chem.* **1995**, *72*, 187; *C. R. Acad. Sci. Série C* **1998**, *1*, 1.
(6) Haouas, M.; Gérardin-In, C.; Taulelle, T.; Estournes, C.; Loiseau, T.; Férey, G. *J. Chem. Phys.* **1998**, *95*, 302.
(7) Cavellec, M.; Riou, D.; Grenèche, J.-M.; Férey, G. *J. Magn. Magn. Mater.* **1996**, *163*, 173.
(8) Cavellec, M.; Egger, C.; Linares, J.; Nogues, M.; Varret, F.; Férey, G. *J. Solid State Chem.* **1997**, *134*, 349.
(9) Cavellec, M.; Riou, D.; Férey, G. *Eur. J. Solid State Chem.* **1995**, *32*, 271.
(10) Cavellec, M.; Grenèche, J.-M.; Riou, D.; Férey, G. *Microporous Mater* **1997**, *8*, 103.
(11) Cavellec, M.; Riou, D.; Ninclaus, C.; Grenèche, J.-M.; Férey, G. *Zeolites* **1996**, *17*, 250.
(12) Cavellec, M.; Grenèche, J.-M.; Férey, G. *Microporous and Mesoporous Mater.* **1998**, *20*, 45.
(13) Lii, K.-H.; Huang, Y.-F. *Chem. Commun.* **1997**, 839.
(14) Lii K.-H.; Huang, Y.-F. *Chem. Commun.* **1997**, 1311.
(15) Lii, K.-H.; Huang, Y.-F. *J. Chem. Soc., Dalton Trans.* **1997**, 2221.
(16) Debord, J. R. D.; Reiff, W. M.; Warren, C. J.; Haushalter, R. C.; Zubieta, J. *Chem. Mater.* **1997**, *9*, 1994.

S0897-4756(98)00108-2 CCC: $15.00
Published on Web 08/14/1998

Table 1. Crystal Data and Structure Refinement for $[Fe_5F_3(PO_4)_6(H_2O)_3](H_2O)_2$, $(H_3N(CH_2)_4NH_3)_3$ (MIL-4)

empirical formula	$[Fe_5F_3(PO_4)_6(H_2O)_3](H_2O)_2 \cdot (H_3N(CH_2)_4NH_3)_3$
formula weight	1266.67 g/mol
temperature	293(2) K
wavelength (Mo Kα)	0.71073 Å
crystal system	orthorhombic
space group	$P2_12_12_1$ (No. 19)
unit cell dimensions	$a = 9.58520(10)$ Å
	$b = 15.5879(3)$ Å
	$c = 29.2556(2)$ Å
volume, Z	4371.17(10) Å^3, 4
density (calcd)	1.925 g cm^{-3}
absorption coefficient	19.49 cm^{-1}
$F(000)$	2580
crystal size	0.23 × 0.2 × 0.04 mm
θ range for data collection	3.35−32.51°
limiting indices	$-12 \le h \le 13$
	$-16 \le k \le 22$
	$-38 \le l \le 44$
reflections collected	36 266
independent reflections	14 514 [R(int) = 0.0430]
refinement method	full-matrix least-squares on F^2
data/restraints/parameters	14 514/0/554
goodness-of-fit on F^2	1.111
final R indices [$I > 2\sigma(I)$]	$R_1 = 0.0601$, $wR_2 = 0.1633$
final R indices [$I > 3\sigma(I)$]	$R_1 = 0.0558$, $wR_2 = 0.1585$ for 11 928 reflections
absolute structure parameter	0.03(2)
extinction coefficient	0.0020(3)
largest diff peak and hole	1.732 and −0.677 e Å^{-3}

99%+), P_2O_5 (Prolabo, 97%), fluorhydric acid HF (Prolabo RP Normapur, 48%, 4.6 M), 1,4-diaminobutane (Aldrich, 99%), and deionized water. The molar ratios were 1:1:2:1.5:80. The mixture was sealed in a 23 mL Teflon-lined Parr acid digestion bomb and heated at 453 K for 72 h. The initial pH was 3, the final one reached 4. At the completion of the synthesis, the resulting product was filtered off, washed with water, and dried in air at room temperature. It consists of a mixture of a few light yellow platelets with a wheat-sheave form and unreacted Fe_2O_3.

TGA measurements were performed under N_2 atmosphere using a TA-Instrument type 2050 analyzer. The heating rate was 5 °C/min from 30 to 600 °C.

2. X-ray Structural Determination. From the bulk material, a suitable single crystal was isolated for data collection on a Siemens SMART three-circle diffractometer equipped with a bidimensional CCD detector. Conditions of data measurements are summarized in Table 1. An absorption correction peculiar to the CCD detector was applied to all data using the SADABS program.[17]

The structure of $[Fe_5F_3(PO_4)_6(H_2O)_3](H_2O)_2 \cdot (N_2C_4H_{14})_3$ was solved by direct methods using the TREF option of the SHELX-TL crystallographic software package. The heaviest atoms (5 Fe + 6 P) were first located. The positions of remaining atoms (O, C, N) were deduced from Fourier-difference maps. Those of fluorine atoms and water molecules were assigned both from bond valence and thermal factor considerations. Geometrical constraints were applied to locate hydrogen atoms. Only the hydrogen atoms of the diamine 1 (see labels of Table 2) have been assigned. Indeed, the thermal agitation of the diamines 2 and 3 was too large to attempt reasonably to find the location of their hydrogen atoms. All non-hydrogen atoms were refined anisotropically; hydrogen atoms were refined with a common isotropic factor. The refinement was led with 14 514 reflections ($I = 2\sigma(I)$) down to $R_1(F_o) = 0.0601$ and $wR_2(F_o^2) = 0.1633$; considering the 11 928 reflections with $I = 3\sigma(I)$, the reliability factors fall to $R_1(F_o) = 0.0558$ and $wR_2(F_o^2) = 0.1585$.

The atomic coordinates and the values of the principal bond lengths are given in Tables 2 and 3, respectively. The anisotropic displacement parameters and the $F_o - F_c$ listings are available on request to the authors.

Table 2. Atomic Coordinates (×10^4) and Equivalent Isotropic Displacement Parameters (Å^2 × 10^3) for MIL-4

atoms	x	y	z	U(eq)[a]
Fe(1)	4748(1)	7656(1)	2235(1)	18(1)
Fe(2)	2713(1)	1436(1)	2116(1)	19(1)
Fe(3)	5232(1)	9296(1)	3177(1)	19(1)
Fe(4)	9729(1)	0088(1)	2491(1)	20(1)
Fe(5)	8682(1)	9673(1)	3679(1)	26(1)
P(1)	7127(1)	0976(1)	3032(1)	18(1)
P(2)	7558(1)	8533(1)	2768(1)	19(1)
P(3)	2933(1)	9423(1)	2390(1)	20(1)
P(4)	4444(1)	7303(1)	3311(1)	19(1)
P(5)	5757(2)	9838(1)	4214(1)	37(1)
P(6)	0103(2)	0839(1)	1459(1)	37(1)
F(1)	1100(3)	1066(2)	2531(1)	24(1)
F(2)	6117(4)	6687(2)	2334(1)	32(1)
F(3)	0033(3)	9874(2)	3166(1)	31(1)
O(1)	4786(5)	8213(2)	3500(1)	26(1)
O(2)	3396(4)	0232(2)	2138(2)	27(1)
O(3)	5877(4)	0391(2)	2904(2)	24(1)
O(4)w	9655(5)	8600(3)	3791(2)	38(1)
O(5)	7391(4)	8998(2)	3240(1)	22(1)
O(6)	7739(4)	0724(2)	3500(1)	25(1)
O(7)	3842(4)	7363(2)	2828(1)	24(1)
O(8)	6017(3)	8541(2)	2596(1)	22(1)
O(9)	1334(4)	9327(2)	2385(2)	26(1)
O(10)	5778(4)	6763(3)	3317(1)	27(1)
O(11)	3530(4)	8655(2)	2123(2)	26(1)
O(12)	8250(4)	0904(2)	2652(1)	24(1)
O(13)	8492(4)	9057(2)	2451(2)	26(1)
O(14)	3362(4)	6912(2)	1928(1)	24(1)
O(15)	3434(4)	9429(2)	2888(2)	24(1)
O(16)	7203(6)	9442(3)	4148(2)	38(1)
O(17)	9402(4)	0347(3)	1841(2)	28(1)
O(18)w	5650(5)	7858(3)	1663(2)	33(1)
O(19)	3375(5)	6882(3)	3628(2)	35(1)
O(20)	1509(5)	1201(3)	1583(2)	36(1)
O(21)w	9902(6)	0200(4)	4103(2)	46(1)
O(22)	4919(5)	9869(3)	3760(2)	32(1)
O(23)	8093(4)	7622(2)	2830(2)	28(1)
O(24)	4916(8)	9215(6)	4537(2)	76(2)
O(25)	5839(8)	0705(5)	4440(3)	74(2)
O(26)	0190(13)	0279(7)	1039(3)	133(5)
O(27)	9191(7)	1628(7)	1326(4)	133(5)
Ow	0956(6)	7582(4)	2728(3)	67(2)
Ow2	4205(17)	7357(7)	920(4)	135(5)
N(1a)	7481(7)	7563(3)	4006(2)	36(1)
N(1b)	2326(7)	8569(6)	4086(2)	62(2)
C(1a)	7627(10)	7191(8)	4461(3)	64(3)
C(1b)	6280(10)	6931(7)	4672(3)	59(2)
C(1c)	1438(11)	8567(7)	4887(3)	59(2)
C(1d)	2138(11)	8025(6)	4517(3)	57(2)
N(2a)	6267(7)	0058(6)	1833(2)	53(2)
N(2b)	8579(14)	0948(8)	4792(3)	92(3)
C(2a)	6393(24)	9654(11)	1406(6)	135(8)
C(2b)	3850(39)	4853(14)	3987(6)	221(18)
C(2c)	6289(40)	9313(12)	562(7)	201(15)
C(2d)	8832(35)	0392(18)	5219(6)	185(12)
N(3a)	7425(11)	6008(7)	1538(3)	72(3)
N(3b)	2065(18)	8450(17)	1281(6)	176(9)
C(3a)	7919(19)	6599(11)	1206(6)	110(6)
C(3b)	1010(28)	2140(20)	3511(13)	199(13)
C(3c)	9952(38)	7635(25)	1200(7)	205(15)
C(3d)	0600(30)	8204(12)	1531(10)	154(9)

[a] U(eq) is defined as one-third of the trace of the orthogonalized U_{ij} tensor.

3. Mössbauer Study and Magnetic Measurements. A sufficient amount of MIL-4 crystals was isolated to perform Mössbauer experiments and magnetic measurements.

Mössbauer experiments were carried out at 300, 77, 4.2, and 2 K using a constant acceleration spectrometer and a ^{57}Co

(17) SADABS program: Siemens Area Detector Absorption Corrections, Sheldrick G. (unpublished).

(18) Teillet, J.; Varret, F. MOSFIT program, Université du Maine (Unpublished).

Table 3. Principal Bond Lengths (Å) for $[Fe_5F_3(PO_4)_6(H_2O)_3](H_2O)_2\cdot(H_3N(CH_2)_4NH_3)_3$ or (MIL-4)

Fe(1)−O(18)$_w$	1.910(4)	Fe(2)−O(20)	1.975(4)	Fe(3)−O(15)	1.930(4)
Fe(1)−O(11)	1.974(4)	Fe(2)−O(2)	1.989(4)	Fe(3)−O(22)	1.950(4)
Fe(1)−O(14)	1.980(4)	Fe(2)−O(10)	1.989(4)	Fe(3)−O(3)	1.982(4)
Fe(1)−O(7)	1.993(4)	Fe(2)−F(2)	1.998(4)	Fe(3)−O(1)	1.983(4)
Fe(1)−F(2)	2.022(4)	Fe(2)−O(23)	2.010(4)	Fe(3)−O(5)	2.130(4)
Fe(1)−O(8)	2.122(4)	Fe(2)−F(1)	2.048(3)	Fe(3)−O(8)	2.199(4)
Fe(4)−O(12)	1.963(4)	Fe(5)−O(21)$_w$	1.892(4)		
Fe(4)−O(9)	1.968(4)	Fe(5)−O(6)	1.944(4)		
Fe(4)−O(17)	1.970(4)	Fe(5)−O(4)$_w$	1.943(4)		
Fe(4)−O(13)	2.000(4)	Fe(5)−O(16)	2.005(5)		
Fe(4)−F(1)	2.016(3)	Fe(5)−F(3)	2.008(4)		
Fe(4)−F(3)	2.022(4)	Fe(5)−O(5)	2.070(4)		
P(1)−O(14)	1.535(4)	P(2)−O(23)	1.521(4)	P(3)−O(2)	1.526(4)
P(1)−O(6)	1.541(4)	P(2)−O(13)	1.526(4)	P(3)−O(15)	1.535(4)
P(1)−O(3)	1.552(4)	P(2)−O(8)	1.560(4)	P(3)−O(9)	1.540(4)
P(1)−O(12)	1.551(4)	P(2)−O(5)	1.568(4)	P(3)−O(11)	1.540(4)
P(4)−O(7)	1.530(4)	P(5)−O(25)	1.506(6)	P(6)−O(20)	1.504(4)
P(4)−O(19)	1.529(4)	P(5)−O(16)	1.530(6)	P(6)−O(26)	1.509(7)
P(4)−O(10)	1.531(4)	P(5)−O(22)	1.552(5)	P(6)−O(17)	1.513(4)
P(4)−O(1)	1.556(4)	P(5)−O(24)	1.577(6)	P(6)−O(27)	1.559(8)
N(1a)-C(1a)	1.46(1)	N(2a)-C(2a)	1.41(2)	N(3a)-C(3a)	1.42(2)
N(1b)-C(1d)	1.53(1)	N(2b)-C(2d)	1.54(2)	N(3b)-C(3d)	1.63(3)
C(1a)-C(1b)	1.49(1)	C(2a)-C(2b)	1.21(3)	C(3a)-C(3b)	1.57(3)
C(1c)-C(1d)	1.53(1)	C(2b)-C(2c)	1.57(2)	C(3b)-C(3c)	1.47(4)
C(1b)-C(1c)	1.52(1)	C(2c)-C(2d)	1.11(3)	C(3c)-C(3d)	1.45(4)

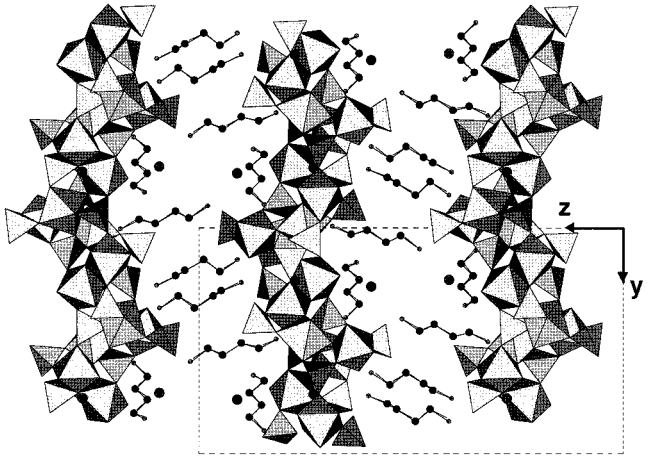

Figure 1. Projection of the bidimensional structure of MIL-4 along [100].

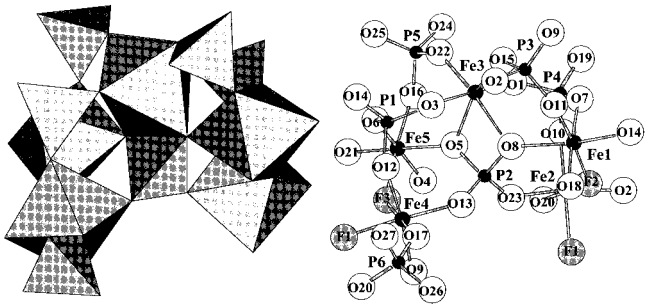

Figure 2. A complex structural unit with an Fe_5P_6 stoechiometry. Polyhedral and ball and stick representations.

source diffused into a Rh matrix. The values of the isomer shifts are quoted relative to α-Fe foil at 300 K. The hyperfine parameters were refined using a least-squares fitting procedure in MOSFIT program.[18]

The magnetization, *M*, of the sample was measured as a function of the applied field, *H* (*H* = 9000 G), at many temperatures in the range 4−300 K with a SQUID (Spin Quantum Interferometer Design). The resulting magnetic susceptibility ($\delta M/\delta H$) was deduced.

Results and Discussion

1. Structural Description. $[Fe^{III}_5F_3(PO_4)_6(H_2O)_3](H_2O)_2\cdot(H_3N(CH_2)_4NH_3)_3$ (MIL-4) presents a bidimensional framework (Figure 1) characterized by the alternation along [001] of organic and inorganic layers strongly related by hydrogen bonds. The inorganic layers are solely built up from the connections by the corners of a unique type of complex structural unit (Figure 2), the central core of this latter being constituted by one $Fe(3)O_6$ octahedron and one $P(2)O_4$ tetrahedron sharing the O(5)−O(8) edge (2.406(5) Å). On this peculiar tetrahedron are added two similar octahedral dimers constituted by one FeO_5F octahedron [Fe(1)$O_4(H_2O)F$ or Fe(5)$O_3(H_2O)_2F$] sharing its fluorine apexes with an FeO_4F_2 octahedron [Fe(2)O_4F_2 or Fe(4)O_4F_2]. In the FeO_4F_2 octahedra, the fluorine apexes are cis-located and F(1) is linked to Fe(4) and Fe(2), thus leading to helicoidal chains of iron octahedra along the mean direction [010] (Figure 3). On the hexameric polyhedral unit are grafted five different PO_4 tetrahedra; whereas $P(1,3)O_4$ present no free apex, $P(4)O_4$ and $P(5,6)O_4$ present one and two terminal oxygen atoms,

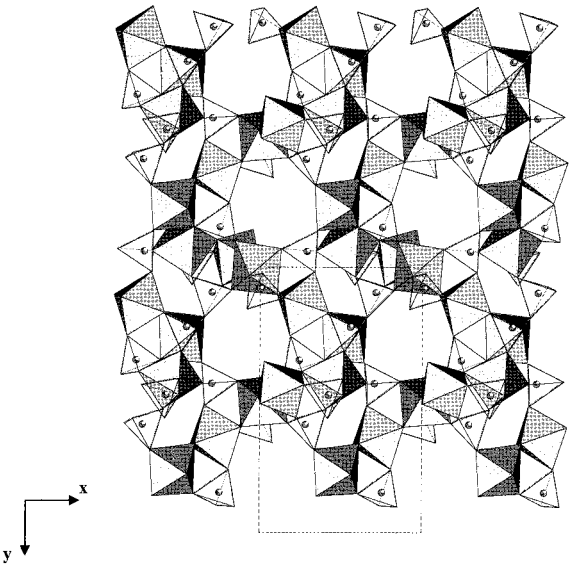

Figure 3. Projection of an inorganic layer along [001].

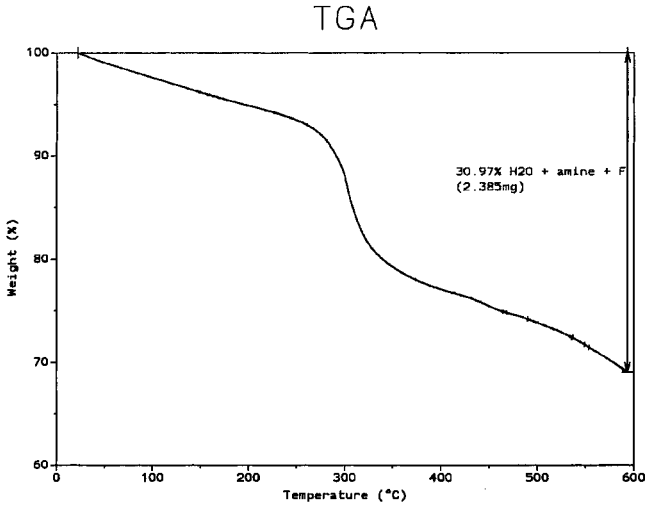

Figure 4. TGA curve performed under a N_2 atmosphere.

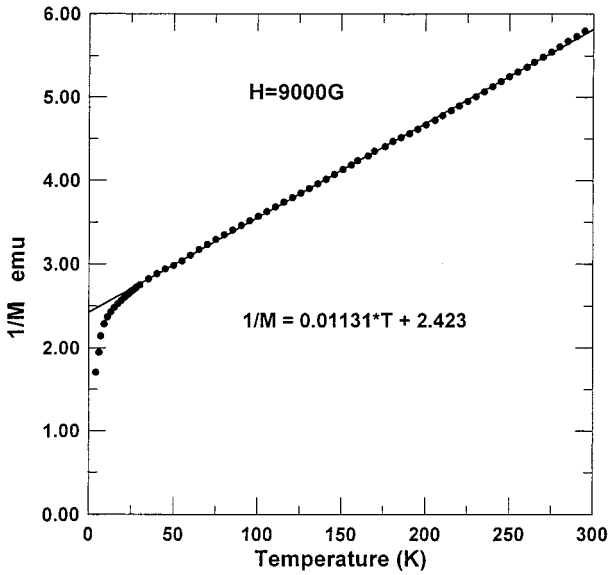

Figure 5. Inverse magnetic susceptibility curve versus temperature.

respectively (Table 3). The ondulated shape of the inorganic layers (Figure 1) generates two kinds of cavities. In the small ones are located the diamines 1; the larger ones contain diamines 2 and 3 and water molecules O_w and O_{w2}. Numbers 1, 2, and 3 correspond to the labels of C and N atoms of Table 2. This situation explains the important distortions observed in the diamines 2 and 3 compared to those of the diamine 1.

TGA results (Figure 4) indicate an experimental loss of around 31% (but it continues beyond 600 °C); it probably corresponds to the whole departure of water + fluorine + amines ($\%_{theor}$ = 32.9%), thus leading to the collapse of the MIL-4 structure.

2. Magnetic Properties and Mössbauer Results. The inverse magnetic susceptibility of $[Fe^{III}_5F_3(PO_4)_6(H_2O)_3](H_2O)_2\cdot(H_3N(CH_2)_4NH_3)_3$ is plotted versus temperature in Figure 5. It is characteristic of a ferrimagnetic compound with a magnetic ordering temperature T_C close to 7 K. The curve followed the Curie−Weiss law in the paramagnetic state (for $T > 35$ K), and the asymptotic Curie−Weiss temperature θ_p is strongly negative ($\theta_p = -214$ K). This is consistent with strong antiferromagnetic superexchange interactions.

Some of the Mössbauer spectra recorded in the paramagnetic (300 and 77 K) and in the magnetic state (2 and 4.2 K) are illustrated in Figures 6 and 7, respectively.

(a) In the *paramagnetic state*, the spectra exhibit symmetrical and well-resolved doublets with slightly broadened but non-Lorentzian lines, indicating (a) that all iron sites have the same coordination and (b) a good crystalline quality. Indeed, the line shape of the spectra is not well-reproduced with only one quadrupolar component with Lorentzian lines.

A first refinement with one quadrupolar contribution did not perfectly reproduced the experimental spectrum. Consequently, in agreement with the crystallographic data, two different fitting procedures were tested (Figure 6): (i) the spectra were fitted with five different quadrupolar components, Γ_i, in order to be correlated to the five crystallographic Fe^{3+} sites, and (ii) the spectra were fitted using three different quadrupolar components taking into account the distortion of the iron octahedra. Indeed, the distortion Δ of each octahedron was calculated using Shannon's formula:[19]

$$\Delta = \frac{1}{i}\sum_i \left[\frac{(x_i - \bar{x})}{\bar{x}}\right]^2$$

with x_i = the distance from cation to anion i and $\bar{x}$ = the mean cation−anion distance.

From the calculations reported in Table 4, one can distinguish three kinds of octahedral units: Fe(2) and Fe(4) octahedra have similar small distortions, Fe(1) and Fe(5) octahedra are much more distorted, and the central Fe(3) octahedron is the only one which is very distorted. These results suggested, a priori, three different types of iron sites which were correlated to three different quadrupolar components.

In both cases (i) and (ii), each component ratio (%) was imposed and the line widths at half-height (Γ) were fitted with an unique value.

Refinement results performing in the first case i are reported in Table 5. Each component ratio was fixed to 20%, in agreement with structural determination. Isomer shift values (IS) are consistent with the presence of high spin state Fe^{3+} ions in octahedral sites. Contrary to oxyfluorinated ferric phosphates previously studied, the similarity of isomer shift values prevents one from distinguishing iron sites according to their anionic neighboring, because of the nature of the hyperfine structure. In addition, one observes slight temperature deviations of the quadrupolar splitting values (QS) for each iron site, but the mean value of the quadrupolar splitting remains strictly temperature and fitting procedure independent (0.75 mm/s). Neverthless, one may discuss the attribution of iron sites according to the quadrupolar splitting values. Indeed, the values of quadrupolar splitting indicate that the component Γ_5 may correspond to the highest distorted site, i.e., the central Fe(3) site (the higher is the distortion of the polyhedra, the higher is the quadrupolar splitting[20]). However, it is quite difficult to

(19) Shannon, R. D. *Acta Crystallogr.* **1976**, *A32*, 751.
(20) Greenwood, N. N.; Gibb, T. C. *Mössbauer Spectroscopy*; Chapman and Hall: London, 1971.

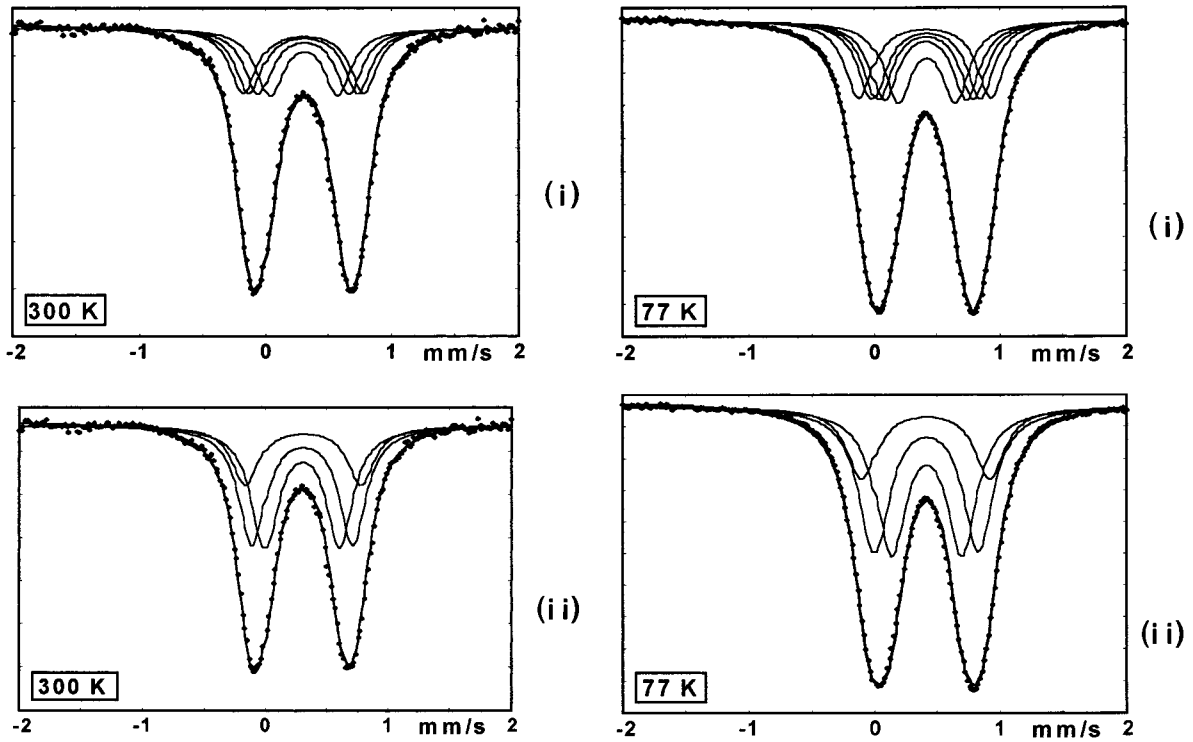

Figure 6. Mössbauer spectra in the paramagnetic state at 300 and 77 K. The spectra are fitted assuming (i) five components (we only see four components because Γ_2 and Γ_3 are superimposed; see the similar hyperfine parameters in Table 5) and (ii) three components, taking into account the distortion of iron octahedra (see text).

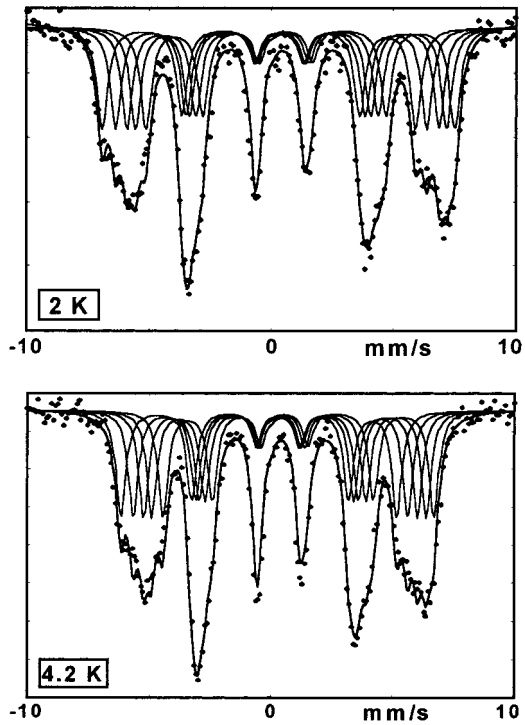

Figure 7. Mössbauer spectra in the magnetic state at 2 and 4.2 K with five components.

attribute the remaining components to the four remaining Fe^{3+} sites.

The second idea (ii) was to associate the iron sites which exhibit similar distortions. Following this thinking, [Fe(1) + Fe(5)] were associated, idem for [Fe(2) + Fe(4)], while Fe(3) remains alone. Spectra were then fitted with three components whose ratios were respectively fixed to 40%, 40%, and 20%. Hyperfine parameters are reported in Table 6. They show that whatever the temperature (300 or 77 K), the component Γ_3 owns the highest quadrupolar splitting and then corresponds to the highest distorted site, i.e., Fe(3) ($\Delta_3 \cdot 10^4 = 23.9$). Then comparing the components Γ_1 and Γ_2, Γ_2 has the highest quadrupolar splitting, so Γ_2 may correspond to [Fe(1) + Fe(5)] ($\Delta_{1,5} \cdot 10^4 = 10$). Thus Γ_1 would be attributed to [Fe(2) + Fe(4)] ($\Delta_{2,4} \cdot 10^4 = 1.4$). So both fitting procedures performed in the paramagnetic state lead to rather similar solutions consistent with crystallographic data.

Table 4. Calculations of the Distortion Δ of the Octahedral Sites

cation	$\Delta \times 10^4$	cation	$\Delta \times 10^4$
Fe(1)	9.98	Fe(4)	1.35
Fe(2)	1.37	Fe(5)	8.58
Fe(3)	23.9		

Table 5. Hyperfine Parameters in the Paramagnetic State Fit with Five Components

		IS ± 0.02	Γ[b]	QS ± 0.02	%[c]
300 K	Γ_1	0.42	0.27	0.53	20
	Γ_2	0.42	0.27	0.71	20
	Γ_3	0.42	0.27	0.71	20
	Γ_4	0.42	0.27	0.85	20
	Γ_5	0.42	0.27	0.94	20
77 K	Γ_1	0.53	0.27	0.46	20
	Γ_2	0.52	0.27	0.65	20
	Γ_3	0.53	0.27	0.75	20
	Γ_4	0.53	0.27	0.85	20
	Γ_5	0.52	0.27	1.04	20

[a] The fit was performed with five components, in agreement with the crystallographic results. IS = isomer shift (mm/s), Γ = line width at half-height (mm/s), QS = quadrupolar splitting (mm/s), % = ratio of the component Γ_i. [b] Refined with the same value. [c] Fixed.

(b) In the *magnetic state*, below 7 K, hyperfine structure requires the use of at least five magnetic

Table 6. Hyperfine Parameters in the Paramagnetic State Fit with Three Components[a]

		IS ± 0.02	Γ[b]	QS ± 0.02	%[c]
300 K	Γ_1	0.42	0.27	0.60	40
	Γ_2	0.42	0.27	0.81	40
	Γ_3	0.42	0.27	0.93	20
77 K	Γ_1	0.53	0.28	0.56	40
	Γ_2	0.53	0.28	0.82	40
	Γ_3	0.52	0.28	1.01	20

[a] The fit was performed with three components taking into account the distortion of iron octahedra. [b] Refined with the same value. [c] Fixed.

Table 7. Hyperfine Parameters in the Magnetic State[a]

		IS ± 0.02	Γ ± 0.02	2ϵ ± 0.02	H_{hyp}	%[b]
4.2 K	Γ_1	0.54	0.54	−0.185	39.5	20
	Γ_2	0.55	0.42	−0.001	36.6	20
	Γ_3	0.51	0.40	0.060	34.2	20
	Γ_4	0.51	0.42	0.004	31.8	20
	Γ_5	0.54	0.59	−0.021	29.3	20
2 K	Γ_1	0.56	0.52	−0.214	44.6	20
	Γ_2	0.58	0.50	−0.047	42.0	20
	Γ_3	0.56	0.48	0.117	39.6	20
	Γ_4	0.54	0.48	0.036	36.8	20
	Γ_5	0.55	0.66	−0.017	33.9	20

[a] IS = isomer shift (mm/s), Γ = line width at half-height (mm/s), 2ϵ = quadrupolar shift (mm/s), H_{hyp} = hyperfine field (Tesla), % = ratio of the component Γ_i. [b] Fixed value.

components during the fitting procedure. The isomer shift values (Table 7) confirm the previous assignment of Fe^{3+} in octahedral sites. The values of the hyperfine fields observed at 4.2 and 2 K are weaker than those encountered in the other ULM-*n* phases.[21] To explain the lowering obtained in the case of MIL-4, one can suggest first (i) the nonsaturated magnetic state, and probably further phenomena, (ii) the role of magnetic frustration, (iii) less effective ligands, and/or (iv) the low-dimensional behavior of the title compound.

(21) Cavellec, M.; Férey, G.; Grenèche, J.-M. *J. Magn. Magn. Mater.* **1997**, *174*, 109.

(i) The difference of hyperfine fields observed at 4.2 and 2 K (estimated at ≈5 T) and the large value of line widths (even at 2 K) suggest higher hyperfine fields at 0 K (saturated magnetic state), which is also consistent with a rather low Curie temperature (≈6−8 K).

(ii) The larger the ratio $|\theta_p/T_{order}|$ is, the stronger is the frustrated magnetic behavior. In MIL-4, the ratio $|\theta_p/T_{order}| = 21.4$ is extremely high and on the same order of magnitude as the antiferromagnetic compound ULM-19[12] ($|\theta_p/T_{order}| = 25$). Accounting for the presence of PO_4 tetrahedral units, one can conclude that the presence of frustration is essentially due to the competition between superexchange and supersuperexchange interactions through these tetrahedra.

(iii) Because oxygen ions produce less effective superexchange than fluorine, one expects a slight reduction of hyperfine fields with the smallest value $H_{hyp(\Gamma 5)}$ attributed to the $Fe(3)O_6$ octahedron, and the intermediate values probably corresponding to $Fe(1,5)O_5F$ octahedra, while the highest refer to $Fe(2,4)O_4F_2$.

(iv) In addition to frustration, a low-dimensional magnetic behavior, which may be expected from the structure, also originates a reduction of hyperfine fields.

Despite rather complex hyperfine structures, Mössbauer data, which are consistent with crystallographic solution, contribute to the explanation of the magnetic properties. However, the lack of magnetic hyperfine data in a low-temperature range (<1 K) prevents detailed and accurate interpretation of present data. Only the comparison with results obtained on previous oxyfluorinated ferric phosphates allowed us to suggest some magnetic behaviors.

Acknowledgment. The authors are indebted to Dr Marc Noguès (Laboratoire de Magnétisme et d'Optique de Versailles) for magnetic susceptibility measurements.

CM9801082